last step in the LUT construction algorithm, this process of expanding the 2D LUT by "adding on" shifted 1D LUT realisations is repeated *(l × n)* times. By selection of the column corresponding to the leftmost pixel of LUT(1), the code obtains a single string of the (*l × n)* numbers making up the complete LUT. This string of numbers hence contain the entire LUT, only now re-ordered in a way so that it is a single smooth and continuous function. This function corresponds to the input SPSF at *n* times improved sampling, but still containing the observationally induced CCD pixel smoothing.

It can be seen that if a single, or a few, of the individual entries in the 2D LUT grid are missing (by unfortunate locations of cosmics, sky-lines and absorption lines), then a whole row will be missing in the 2D LUT grid. In the continuous high-resolution representation of the LUT, however, a missing entry will only result in a set of single missing values at each 25th sub-pixel. Those can easily be determined via interpolation between good values. After interpolation to determine unknown values, possibly some smoothing if the spectrum in general has low S/N, the process is reversed, and the 2D LUT is reconstructed from the interpolated/smoothed high-resolution representation. This is the last step of a given iteration. If another iteration is started, the new LUT will be used.

4. Degeneracy of Results and Concluding Remarks

We have presented an algorithm that is specifically aimed at performing the best possible removal of a 2D spectrum to reveal faint emission-line objects "hidden" under a bright spectrum. A few notes should be added. **First:** As detailed in Section 2, an algorithm with this goal has to use a global approach to the determination of the SPSF. A global approach is clearly incompatible with the fact that the SPSF varies along the spectrum; some additional assumption is required. In the code described here, we have assumed that the SPSF at any wavelength can be obtained via a linear scaling in width of the same base SPSF. **Second:** Clearly, if two point sources are super-imposed at exactly the same position, there is no way the code can tell that there are in fact two different objects. It will regard the summed spectrum as that of a single point source. **Third:** If the emission-line object is not a point source, and if it extends across the bright point source, the code will try (as a default) to assign as much flux as possible to the point source. This means that part of the emission-line object will be assigned to the spectrum of the bright point source, and the code will "dig a hole" in the extended object at the position of the bright point source. In both of those two cases, there is hence a certain degeneracy in the final solution as to how much flux should be assigned to the two objects. This degeneracy can be broken in several ways. Typically, one may assume that either the spectrum of the point source is smooth and continuous in the given spectral region, or one may assume that the extended object has a smooth and continuous surface brightness distribution at the position of the bright point source. In the case of two compact and well separated objects no additional assumptions are needed, the solution will be unique.

Acknowledgements

I wish to thank Michael I. Andersen who supplied the routines that perform the optimal fitting of Chebyshev polynomials, and Sandra Savaglio who provided extensive comments on several other functionalities of this data-reduction tool. I am grateful to Keith Horne for many useful comments on an earlier version of this report.

References

Horne, K., 1986, *PASP*, **118**, 609.
Marsh, T.R., 1989, *PASP*, **101**, 1032.
Møller, P., Kjærgaard, P., 1992, *A&A*, **258**, 234.
Møller, P., 1999, in *Astrophysics with the NOT,* Karttunen, H. and Piirola, V. (eds.), University of Turku, p. 80-88.
Møller, P., et al., 2000, *The Messenger*, **99**, 33.
Treu, T., Stiavelli, M., Casertano, S., Møller, P., Bertin, G., 1999, *MNRAS*, **308**, 1037.

SPSF Subtraction II: The Extended Lyα Emission of a Radio Quiet QSO

P. MØLLER[1], S.J. WARREN[2], S.M. FALL[3], P. JAKOBSEN[4], J.U. FYNBO[5]

[1]*ESO, Karl-Schwarzschild-Str. 2, Garching, Germany*
[2]*Blackett Laboratory, Imperial College of Science, Technology and Medicine, London, UK*
[3]*Space Telescope Science Institute, Baltimore, USA*
[4]*Astrophysics Division, Space Science Department of ESA, ESTEC, Noordwijk, The Netherlands*
[5]*Institute of Physics and Astronomy, University of Århus, Århus, Denmark*

1. Introduction

A common trait of high-redshift radio galaxies is their extended Lyα emission. This emission-line nebulosity is generally aligned with the radio axis, and similar emission has been reported around radio-loud QSOs (Schneider et al. 1987, Heckman et al. 1991a,b, Hu et al. 1991). For radio-quiet QSOs, it appears that extended Lyα emission is much less common. Hu et al. (1991) found extended emission-line nebulosity around three of ten radio-loud QSOs, but from none of the seven radio-quiet QSOs in their sample. Steidel et al. (1991) and Bergeron et al. (1999) reported the detection of extended Lyα emission from two radio-weak QSOs, and Bremer at al. (1992) reported the so far only detection of extended Lyα emission from a radio-quiet QSO.

Two methods have been used in all of the work quoted above, narrow-band imaging and direct inspection of two-dimensional (2D) CCD spectra to look for regions of emission extending away from the spectrum of the QSO. A tool that would allow modelling and subtraction of the 2D spectrum of the QSO would not only improve the chances of detecting faint emission lines in the vicinity of the QSO, it could also allow more detailed analysis. Our first report on spectral PSF (SPSF) subtraction (Møller, 2000) described a technique for SPSF subtraction. In this second report, as a simple example of an application of the tool, we report the serendipitous discovery of extended Lyα emission from the host galaxy of the radio quiet z = 2.559 QSO Q2206-199.

2. Observations

On August 12, 1999, we obtained four FORS1/Grism 600B long slit spectra, each of 2000 sec integration time, of the radio quiet QSO Q2206-199. Our observing strategy was to obtain several spectra with different offsets along the slit, to minimise the effects of flat-field errors and other systematic effects. This is a crucial point to keep in mind when one is in search of extremely faint features close to, or on top of, a much brighter object.

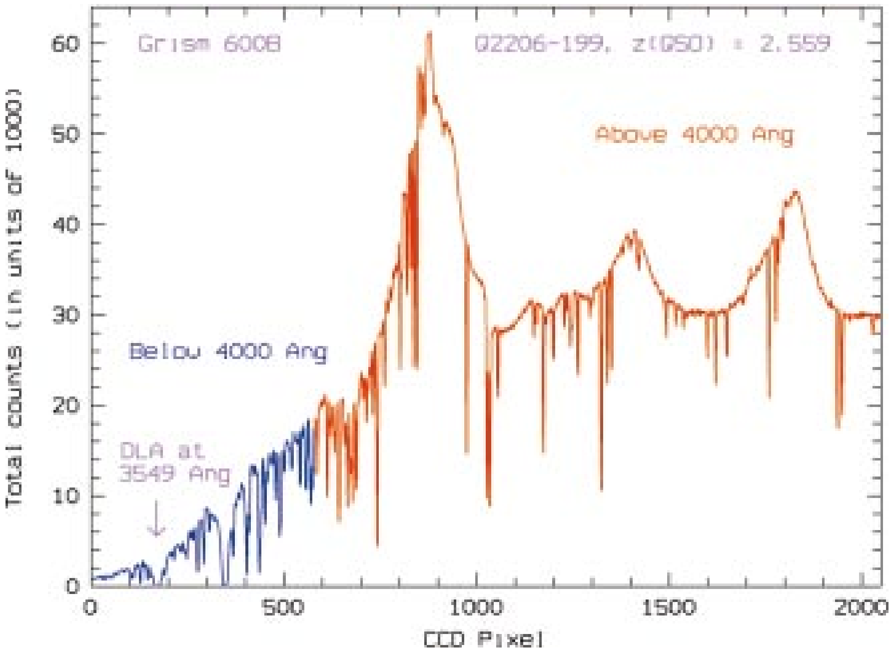

Figure 1: FORS1/600B raw extracted spectrum (8000 seconds) of the z = 2.559 radio quiet QSO Q2206-199.

The spectra were obtained with a PA of 236 deg. and the seeing from the automatic seeing monitor (the DIMM) during all exposures was recorded as 0.40–0.45 arcsec. After flat-fielding, shifting and co-addition of the four individual spectra, the measured combined FWHM of the QSO SPSF along the slit is 0.60 arcsec, which is an acceptable degradation of the SPSF as compared to the imaging PSF.

Following the co-addition we used the code described in Report 1 to perform the tracing of the spectrum, to determine the SPSF as a function of wavelength, and to extract the maximum signal-to-noise spectrum of the QSO. In Figure 1, we present the extracted spectrum. The vertical scale is total CCD counts per bin (the ADU conversion is 1.48 e^-/count). The spectrum is clearly of very high S/N in the region above 4000 Angstrom (red part of the spectrum in Fig. 1), but below 4000 Angstrom (blue part), the combined instrument efficiency drops rapidly. Our target DLA system (at 3549 Angstrom) is deep into the low efficiency part of the spectrum, but despite the low efficiency, we obtained a very clear detection of Lyα emission from the DLA galaxy (to be reported in our third and last SPSF report).

3. Application of SPSF Subtraction: QSO Host Galaxies

The search for the host galaxies of QSOs and the interpretation of their spectral energy distributions has recently started to move from low (z = 0.1–0.3) towards higher (z = 2–3) redshifts, and has become a topic of current debate (Terlevich and Boyle 1993, Aretxaga et al. 1998, Fynbo, Burud and Møller 2000). A proposal as to how one may detect extended line emission across QSO spectra was recently presented by Courbin et al. 1999. Spectroscopic detection of emission lines from the QSO host galaxies would be an important step forward, as it would clarify many of the current questions concerning the high redshift QSOs and their host galaxies.

1. **Is the redshift of the host galaxy the same as that of the QSO broad Lyα and CIV lines?** It has long been known that the QSO high ionisation lines are significantly blue shifted with respect to the low ionisation lines. The low ionisation lines are expected to represent the true systemic redshift of the QSO (Espey et al. 1989, Corbin 1990, Møller, Warren and Fynbo 1998). Emission lines from the host galaxy should be found at the systemic redshift, hence they should be redshifted from the broad Lyα and CIV of the QSO.

2. **What is the velocity width of the extended line emission?** If the emission from the QSO host galaxy is in reality caused by simple dust reflection (see e.g. Fynbo, Burud and Møller 2000) of the QSO spectrum, such as has been reported for radio galaxies, then the host galaxy spectrum must have both Lyα redshift and line velocity widths identical to that of the QSO itself. If that is not the case then one can rule out the dust-reflection hypothesis.

3. **What is the dynamical mass of the QSO host galaxy?** If the extended line emission is not due to reflected QSO light, then the velocity profile over the spatial extent of the line emission reflects the dynamical state of the emitting gas. It may even be possible to determine a rotation curve. This could provide limits on the mass of the dark matter halos in which the high redshift quasars form.

Data of the quality shown in Figure 1 with high S/N at Lyα, excellent seeing and good sampling of the SPSF, clearly provide the best possible conditions to address those questions. In Figure 2 we show (left panel) a section of the 2D QSO spectrum centred on the Lyα emission line of the QSO. After maximum S/N extraction of the 1D spectrum as described above, we subtracted the minimum χ^2 fit of the 2D spectrum. For illustration purposes, we have (central panel of Fig. 2) only subtracted the central part of the fitted QSO spectrum. The residuals clearly show evidence for extended Lyα emission. The rightmost panel of Figure 2 shows the residuals after the PSF subtraction and after simple box-car smoothing to enhance the contrast of the extended emission over the background noise.

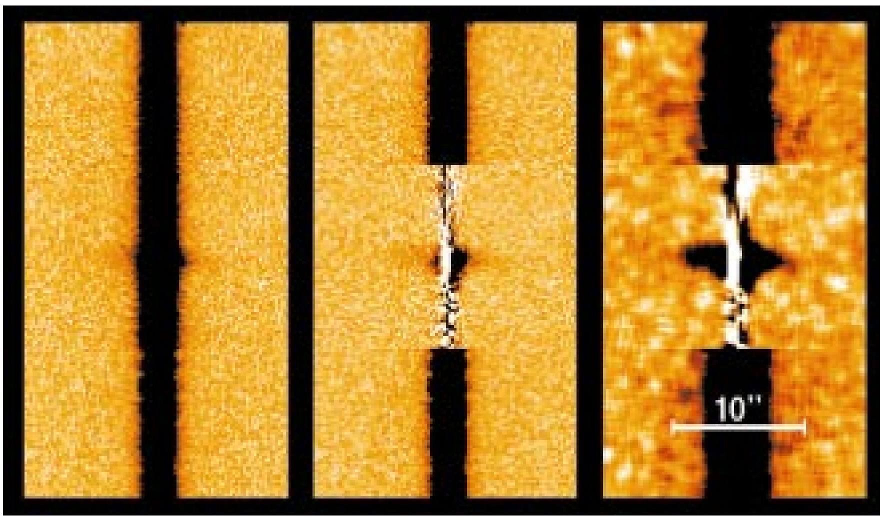

Figure 2: 2D spectrum covering the region around Lyα. ***Left:*** *2D spectrum after sky subtraction.* ***Centre:*** *2D spectrum after sky subtraction and subtraction of the minimum χ^2 fit of the central part of the 2D QSO spectrum.* ***Right:*** *Same as the spectrum in the centre but after simple box-car smoothing to enhance the contrast of the extended emission over the background noise. The horizontal scale (along the slit) in all three panels is 0.2 arcsec per pixel.*

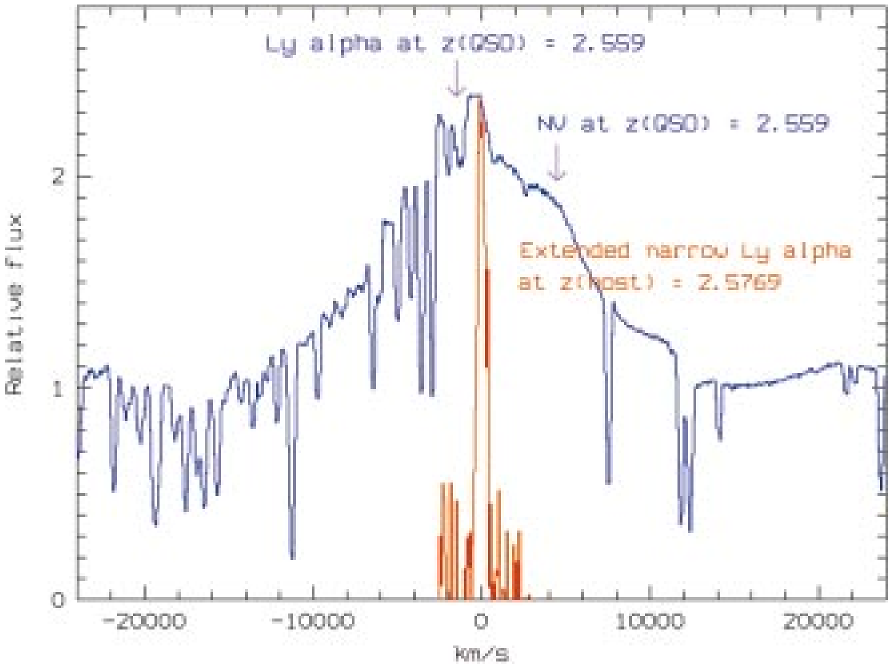

Figure 3: ***Blue:*** *Spectrum of the Lyα line region of the QSO Q2206-199 normalised to 1 in the continuum.* ***Red:*** *Spectrum of the extended Lyα line of the host galaxy of Q2206-199. Note that the extended Lyα is much narrower than the QSO Lyα, and that the QSO emission-line redshift is blue shifted by 1500 km/s. The extended Lyα amplitude was scaled arbitrarily for easy comparison to the QSO spectrum.*

Clearly, we detect extended Lyα emission over a region of almost 10 arcsec (roughly 50 h^{-1} kpc), and the three questions asked above can now be addressed.

4. Extended Lyα of a High-Redshift QSO Host Galaxy

The CCD columns very close to the central part of the 2D spectrum show large residuals at all wavelength bins. This is due to the large photon shot-noise. Faint objects cannot ever be detected close to the central part of the QSO SPSF because of this. To obtain the spectrum of the extended host galaxy we therefore ignored the central noisy columns, and averaged the regions left and right of the residuals of the middle frame of Figure 2. This spectrum is plotted in red in Figure 3. Also in Figure 3, we have plotted the normalised spectrum of the broad Lyα and NV lines of the QSO Q2206-199. The expected position of the quasar emission lines (for z_{QSO} = 2.559) are marked in Figure 3. The emission redshift of Q2206-199 is taken from the literature and is based on the Lyα, SiIV, and CIV emission lines.

It is immediately clear that the broad lines of the QSO are blue shifted by 1500 km/s with respect to the extended Lyα, and also that the extended Lyα is much narrower than the broad QSO Lyα line. Those two observations confirm that the extended Lyα is indeed at the systemic redshift of the QSO and must be the signature of gas in the host galaxy. It is not caused by dust reflection of quasar light. The FWHM of the narrow Lyα is 760 km/s (at PA 236 deg E of N) and 510 km/s (at PA 56 deg E of N). It is interesting to note that there is no hint of Lyα absorption at the redshift of the host galaxy.

From visual inspection of Figure 2 (right frame) it appears that the extended Lyα cloud is rotating. We shall now quantify this observation. For each CCD column where the extended Lyα was strong enough, we fitted a gaussian to the velocity profile. Also here, we ignored the noise-dominated columns close to the central part of the QSO spectrum. The centroids of the velocity profiles, as a function of the projected distance from the QSO, are plotted in Figure 4. It is clear from Figure 4 that the host galaxy gas is indeed rotating. With only a single slit orientation, we cannot know if we are on the major or minor axis of the host galaxy or somewhere in between, and we also do not know what the inclination angle of the galaxy is. Hence, the apparent rotation velocity of about 50–100 km/s at a projected radius of about 25h^{-1} kpc, is a lower limit, which places a lower limit of a few times 10^{10} h^{-1} Solar masses on the dynamical mass inside this radius. The most striking result from Figure 4 is, however, that the rotation velocity appears to keep growing outwards. Hence, there is likely a significant amount of mass located at even larger distances from the central QSO. This would support the view that QSOs at high redshifts are formed in deep potential wells.

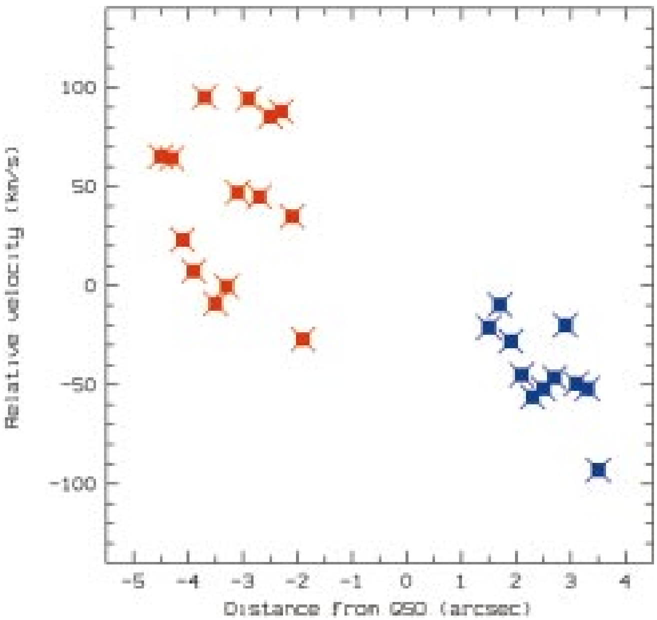

Figure 4: Relative projected motion of the host galaxy gas. The data clearly indicate rotation.

Acknowledgements

Based on observations collected at the European Southern Observatory, Paranal, Chile (ESO Programme 63.0-0618).

References

Aretxaga I., Terlevich R.J., Boyle B.J., 1998, *MNRAS* **296**, 643.

Bergeron, J., Petitjean, P., Cristiani, S., Arnouts, S., Bresolin, F., Fasano, G., 1999, *A&A* **343**, L40.

Bremer M.N., Fabian A.C., Sargent W.L.W., Steidel C.C., Boksenberg A., Johnstone R.M., 1992, *MNRAS* **258**, L23.

Corbin, M.R., 1990, *ApJ*, **357**, 346.

Courbin, F., Magain, P., Sohy, S., Lidman, C., Meylan, G., 1999, *The Messenger*, **97**, 26.

Espey, B.R., Carswell, R.F., Bailey, J.A., Smith, M.G., Ward, M.J., 1989, *ApJ*, **342**, 666.

Fynbo, J.U., Burud, I., Møller, P., 2000, *A&A*, submitted.

Heckman T.M., Lehnert M.D., van Breugel W., Miley G.K., 1991a, *ApJ* **370**, 78.

Heckman T.M., Lehnert M.D., Miley G.K., van Breugel W., 1991b, *ApJ* **381**, 373.

Hu E.M., Songaila A., Cowie L.L., Stockton A., 1991, *ApJ* **368**, 28.

Møller, P., Warren, S.J., Fynbo, J.U., 1998, *A&A*, **330**, 19.

Møller, P., 2000, *The Messenger*, **99**, 31.

Schneider D.P., Gunn J.E., Turner E.L., Lawrence C.R., Schmidt M., Burke B.F., 1987, *AJ* **94**, 12.

Steidel C.C., Sargent W.L.W., Dickinson M., 1991, *AJ* **101**, 1187.

Terlevich R.J., Boyle B.J., 1993, *MNRAS* **262**, 491.